Comparison of VIIRS Prelaunch RVS among Independent Studies

A. Wu[a], Jeff McIntire[a], X. Xiong[b], F. J. De Luccia[c] and Co-authors

[a]The Sigma Space Corporation, Lanham, MD 20706
[b]Science and Exploration Directorate, NASA/GSFC, Greenbelt, MD 20771
[c]The Aerospace Corporation, P. O. Box 92957 - M8/715, Los Angeles, CA 90009-2957

ABSTRACT

The Visible Infrared Imaging Radiometer Suite (VIIRS) is a key sensor carried on the NPOESS (National Polar-orbiting Operational Environmental Satellite System), upgraded and developed recently from heritage instruments including AVHRR, OLS, MODIS, and SeaWiFS. It has on-board calibration components including a solar diffuser (SD) and a solar diffuser stability monitor (SDSM) for the reflective solar bands (RSB), a V-groove blackbody for the thermal emissive bands (TEB), and a space view (SV) port for background subtraction. These on-board calibrators are located at fixed scan angles. The VIIRS response versus scan angle (RVS) was characterized prelaunch in lab ambient conditions and will be used on-orbit to characterize the response for the all scan angles relative to the calibrator scan angle (SD for RSB and blackbody for TEB). Since the RVS is vitally important to the quality of calibrated radiance products, several independent studies were performed and their results were compared and validated. This document provides RVS results from three groups: the NPP Instrument Calibration Support Team (NICST), Raytheon, and the Aerospace Corporation. A comparison of the RVS results obtained using a 2nd order polynomial fit to measurement data is conducted for each band, detector, and half angle mirror (HAM) side. The associated RVS fitting residuals are examined and compared with the relative differences in RVS found between independent studies. Results show that the agreement is within 0.1% and comparable with fitting residuals for all bands except for RSB band M9, where a difference of 0.2% results from the application of the atmospheric water vapor correction for laboratory conditions during the test by Raytheon. NICST has slightly larger RSB RVS uncertainties but still well within the 0.3% total uncertainty allowed for the RVS characterization defined in the Performance Verification Plan.

Keywords: VIIRS, calibration, prelaunch, response versus scan angle

1. INTRODUCTION

The Visible Infrared Imaging Radiometer Suite (VIIRS) is a key sensor carried on NPOESS (National Polar-orbiting Operational Environmental Satellite System) (http://www.ipo.noaa.gov/index.php?pg=viirs). The NPOESS Preparatory Project (NPP) [1] is

scheduled to launch in October 2011. VIIRS is upgraded and developed from heritage instruments including AVHRR, OLS, MODIS, and SeaWiFS. It uses a constant-rate rotating telescope assembly (RTA) and a double sided half angle mirror (HAM) rotating at half the speed of the RTA. VIIRS has 22 bands with a spectral range from 0.4 to 12.0 µm (see Table 1). The Earth view swath covers a distance of ~3000 km over scan angles ranging from $\pm 56.0^o$ off nadir. Observations by VIIRS cover the entire earth's surface every one or two days and the derived products provide unprecedented information describing land, ocean, and atmosphere.

The on-board calibration components are a solar diffuser (SD) and a solar diffuser stability monitor (SDSM) for the reflective solar bands (RSB), a V-groove blackbody for the thermal emissive bands (TEB), and a space view (SV) port used to remove background signals for both RSB and TEB. The SD and blackbody provide absolute calibration with standards traceable to those provided by the National Institute of Standards and Technology (NIST). Since both the SD and blackbody are located at fixed angles of incidence (AOI), the calibration at other AOIs is dependent upon the response versus scan angle (RVS) relative to the on-board calibrators. Thus, how well the RVS is characterized is vitally important to ensure the quality of the calibrated radiance product.

The VIIRS RVS was characterized prelaunch in lab ambient conditions. These tests were conducted at a number of different scan angles (see Table 2) so a complete description of the RVS was achieved. The purpose of this document is to provide the VIIRS prelaunch RVS results from three independent analyses [2-9] and examine how well they agree. The three RVS results are obtained from the NPP Instrument Calibration Support Team (NICST) funded by NASA, Raytheon, and the Aerospace Corporation. This document provides a comparison of the RVS results for each band, detector, and HAM side. The associated RVS uncertainties are examined and compared with the relative differences found between independent studies.

Table 1. VIIRS sensor spectral bands (units in nm)

RSB			TEB		
Band	**CW**	**BW**	**Band**	**CW**	**BW**
M1	412	20	M12	3700	180
M2	445	18	M13	4050	155
M3	488	20	M14	8550	300
M4	555	20	M15	10763	1000
M5	672	20	M16	12013	950
M6	746	15	I4	3740	380
M7	865	39	I5	11450	1900
M8	1240	20			
M9	1378	15			
M10	1610	60			

M11	2250	50
I1	640	80
I2	865	39
I3	1610	60

2. METHODOLOGY

The RVS tests were performed in lab ambient conditions using the specified methodology [10]. The sensor was in diagnostic mode. During the tests for the RSB, the VIIRS instrument viewed the aperture of a 100 cm spherical integrating source (SIS-100). For the TEB, the SIS-100 was replaced with a fixed blackbody source, the Lab Ambient Blackbody (LABB). All tests were conducted at a number of different scan angles (see Table 2). These scan angles correspond to different angles of incidence (AOI) on the Half Angle Mirror (HAM). The HAM mirror coating is FSS99-500, a Denton silver coating with a protective thin film overcoat. Changes in HAM mirror reflectivity with scan angle are captured by the detector response.

Methods used by the three groups to determine the RSB RVS are similar [3,5,8], in which detector responses are corrected first for the total drift in their measurements during the course of the test due to the inadequacy of the SIS-100 radiance monitor. The drift correction is derived from four repeated measurements of a fixed scan angle of -8.0^o at different times throughout the test. Methods used to determine the TEB RVS are different between Raytheon and other two groups [2,4,6-7,9]. Raytheon used an iterative solution while NICST and Aerospace used a relatively simple approach, in which detector responses are normalized with the LABB source radiance. After these treatments to the original measurement data, a second order polynomial is used to fit the detector response versus AOI, or

$$RVS = a_0 + a_1 AOI + a_2 AOI^2 \qquad (1)$$

Once the coefficients a_0, a_1, and a_2 are produced, equation (1) is used to characterize the RVS for both RSB and TEB for all AOI. These RVS coefficients are band, detector, HAM side, and sub-sample dependent. The VIIRS earth scene AOI range is from 29.0^o to 56.47^o. Since the RVS is characterized relative to the reference, equation (1) is generally normalized to the AOI of the onboard calibrators. For the RSB, the normalization point is the AOI of solar diffuser (SD) at 60.18^o; for the TEB, the RVS is normalized to the AOI of the blackbody at 38.08^o. The RVS results presented in this document are extracted based on equation (1) with coefficients a_0, a_1, and a_2 provided by the three independent studies.

**Table 2**. Scan angles and AOI used during the prelaunch thermal vacuum tests to derive the RVS for RSB and TEB*.

RSB		TEB	
Scan Angle	AOI	Scan Angle	AOI
-65.7	60.5	-65.7	60.5
-55.5	56.2	-60.6	58.3
-51.0	54.4	-55.5	56.2
-45.0	52.0	-51.0	54.4
-38.0	49.3	-45.0	52.0
-30.0	46.2	-38.0	49.3
-20.0	42.6	-30.0	46.2
-8.0	38.5	-20.0	42.6
6.0	34.4	-8.0	38.5
22.0	30.8	6.0	34.4
38.0	28.8	22.0	30.8
55.5	29.0	35.0	29.1

*Note the exact scan angles or AOI used among the three independent studies may be slightly different depending on their selection of the sweet spot center.

3. RESULTS

3.1 Agreement between averages over detectors within a band

RVS results are first evaluated using averaged values over detectors within each band. Figure 1 compares the M1 RVS obtained from NICST, Raytheon, and Aerospace, plotted as a function of AOI over a complete earth view scan (AOI from 29.0^{o} to 56.47^{o}) for HAM sides A and B. Values of the RVS are normalized at AOI = 60.18^{o}, which is the viewing angle for the SD. There is excellent agreement in the RVS with differences of less than 0.1% between any two groups. To better illustrate the agreement, values of the RVS are extracted at three AOI: 1) beginning of scan (BOS) at an AOI of 56.47^{o}, 2) nadir of scan (NOS) at an AOI of 38.53^{o} and 3) end of scan (EOS) at an AOI of 29.0^{o}. Table 3 lists these RVS values at the three AOI for both RSB and TEB. Results show that agreement between groups is within 0.1% for all RSB and TEB except for M9, where a difference of 0.2% is found at BOS. The reason that M9 has a relatively large difference is due to the use of an atmospheric water vapor correction by Raytheon; no correction was applied in the results from NICST and Aerospace. The correction for water vapor is necessary because the wavelength of M9 (1.378 µm) lies within a water absorption region. Even small changes in the water content in the clean room air during the test can significantly affect the detector response.
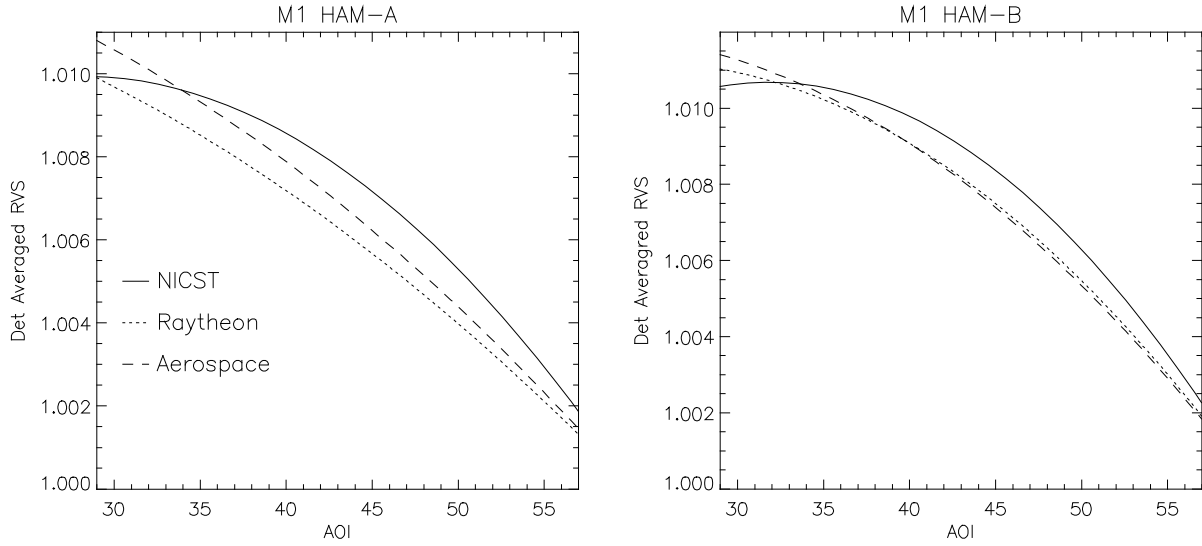
Figure 1. Comparison of detector averaged RVS for M1 at HAM A and B sides using results obtained from NICST, Raytheon, and Aerospace.

Table 3. Comparison of RVS from NICST, Raytheon (RTN), and Aerospace (Aero) at three AOI.

RSB	BOS (AOI=29°)			NOS (AOI=38°)			EOS (AOI=56°)		
	NICST	RTN	Aero	NICST	RTN	Aero	NICST	RTN	Aero
M1	1.010	1.010	1.011	1.009	1.008	1.008	1.002	1.001	1.002
M2	1.008	1.008	1.009	1.007	1.006	1.007	1.001	1.001	1.001
M3	1.006	1.006	1.006	1.004	1.004	1.004	1.001	1.001	1.001
M4	1.005	1.005	1.005	1.003	1.003	1.003	1.000	1.000	1.000
M5	1.005	1.006	1.005	1.004	1.005	1.005	1.001	1.001	1.001
M6	0.999	0.999	0.999	0.999	0.999	1.000	1.000	1.000	1.000
M7	0.995	0.995	0.995	0.996	0.996	0.996	0.999	0.999	0.999
M8	0.998	0.998	0.998	0.998	0.998	0.998	1.000	1.000	1.000
M9	0.998	0.996	0.997	0.998	0.997	0.998	1.000	1.000	1.000
M10	0.999	0.999	0.999	0.999	0.999	0.999	1.000	1.000	1.000
M11	1.001	1.001	1.001	1.001	1.001	1.000	1.000	1.000	1.000
I1	1.007	1.007	1.007	1.005	1.006	1.006	1.001	1.001	1.001
I2	0.994	0.995	0.995	0.996	0.996	0.996	0.999	0.999	0.999
I3	0.999	0.999	0.999	1.000	0.999	1.000	1.000	1.000	1.000
TEB									
M12	1.005	1.005	1.005	1.004	1.004	1.004	1.001	1.001	1.001
M13	1.005	1.005	1.004	1.004	1.004	1.004	1.001	1.001	1.001
M14	1.085	1.086	1.086	1.067	1.068	1.069	1.014	1.014	1.015
M15	1.049	1.049	1.050	1.039	1.040	1.040	1.008	1.008	1.009

M16A	1.028	1.028	1.028	1.022	1.023	1.023	1.005	1.005	1.005
M16B	1.028	1.028	1.028	1.022	1.023	1.023	1.005	1.005	1.005
I4	1.002	1.001	1.001	1.000	1.000	1.000	0.997	0.997	0.997
I5	1.007	1.007	1.006	1.000	1.000	1.000	0.977	0.977	0.977

3.2 Comparison of detector-to-detector differences

Since the RVS of the RSB is normalized at an AOI of 60.18^o and the AOI for BOS is 56.47^o, it is expected that relatively large detector-to-detector differences occur near the EOS region corresponding to small AOI. To better quantify detector-to-detector differences in each band, values of detector-level RVS are divided by the detector mean. Figure 2 plots the M1 RVS normalized with the detector mean using results from NICST, Raytheon, and Aerospace. Results show that the detector-to-detector differences in M1 are within 0.1% and all three independent studies have generally good agreement. Examination of the RVS results among all bands indicates that the largest detector-to-detector difference occurs in M14 (Figure 3), where up to 0.4% differences between detectors are found near the EOS region (AOI $\sim 29.0^o$). Plotting the M14 RVS versus the detector number indicates that there is an upward trend with detector number and a systematic difference of around 0.1% between even and odd detectors (Figure 4). A noticeable increase in RVS with detector number for M14 might be due to the fact this band has the largest change in RVS across the entire scan (~8%). It is still unclear the reason for the RVS difference between even and odd detectors in M14. Analysis of the RVS fitting residuals (see section 3.3) does not suggest that there is a systematic difference between even and odd detectors.
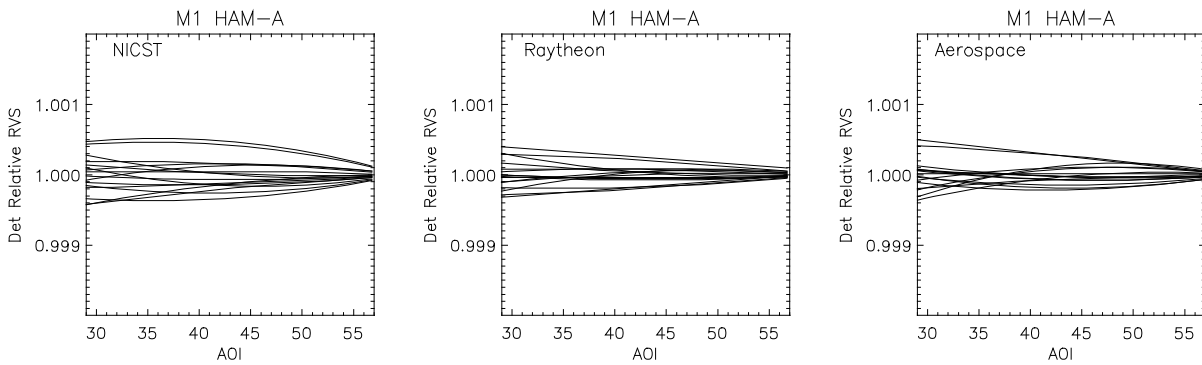
Figure 2. Detector-to-detector relative RVS versus AOI for M1 at HAM side A
obtained from NICST, Raytheon, and Aerospace. There are 16 detectors
for M1.
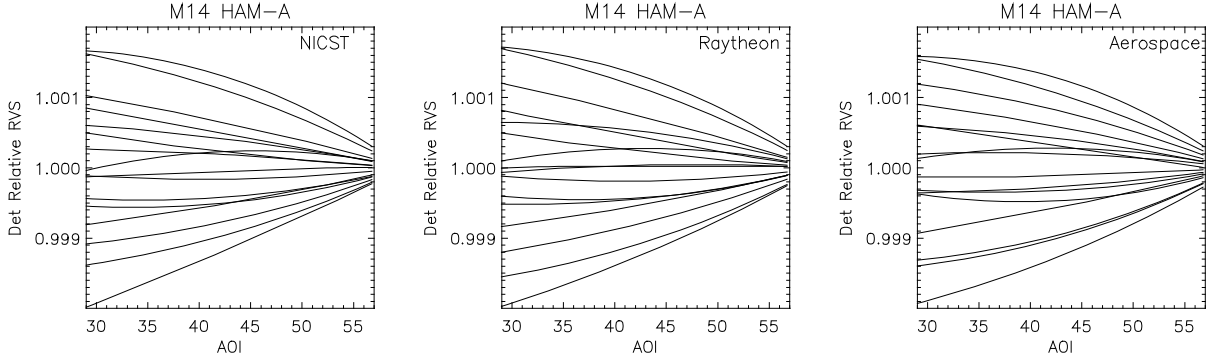
Figure 3. Detector-to-detector relative RVS versus AOI for M14 at HAM side A
obtained from NICST, Raytheon, and Aerospace. There are 16 detectors
for M14.
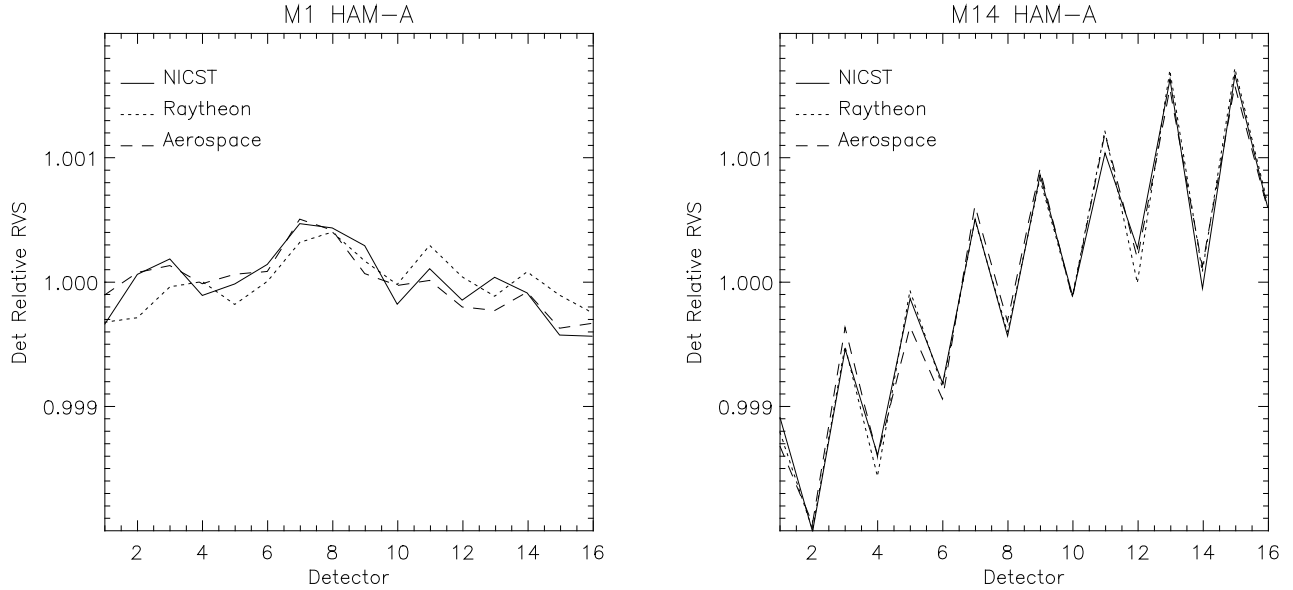
Figure 4. Comparison of detector-to-detector relative RVS versus detector number
for M1 and M14 at HAM side A among results from NICST, Raytheon,
and Aerospace.

3.3 Comparison of fitting residuals

When equation (1) is used to fit a RVS curve, a total fitting residual can be computed, which is
the standard error between the fitting and measured values. Figure 5 compares the fitting
uncertainties in percentage converted from the fitting residuals for the three groups.
Uncertainties from NICST are larger for almost all RSB. As discussed previously, the
exceptionally high residuals for M9 are due to the impact of water vapor during the tests. For the

TEB, the uncertainties obtained from all three independent studies are generally similar, with values being less than about 0.10%. Both RSB and TEB uncertainties are comparable in magnitude with the RVS relative differences found among the three groups. All uncertainties obtained from the three independent studies are within the requirement value of 0.3% allowed for the characterization of the RVS, specified by the Performance Verification Plan (PVP) PVP154640-101 [11].
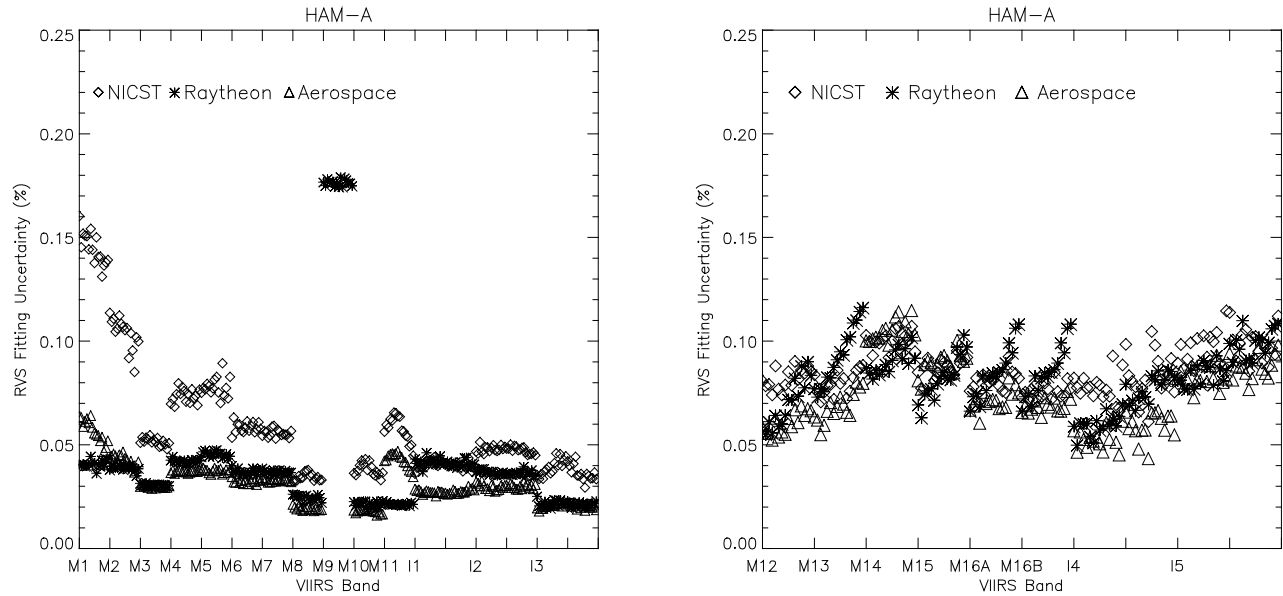
Figure 5. Comparison of the RVS fitting uncertainties (residuals) at the detector level for RSB (left) and TEB (right) using HAM side A among results from NICST, Raytheon, and Aerospace.
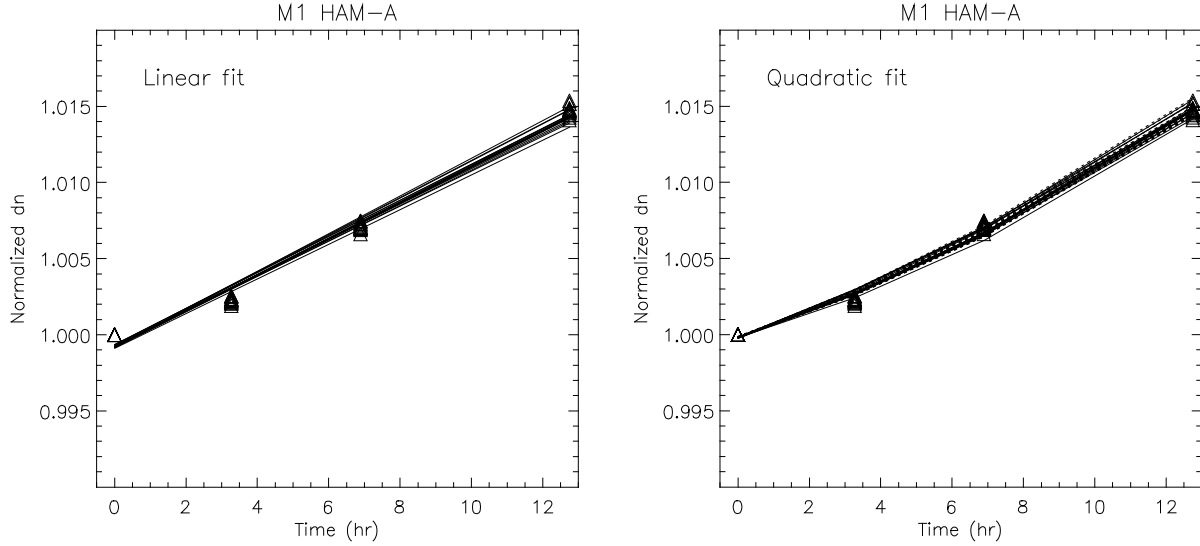
Figure 6. Comparison of the linear (left) and quadratic (right) fits obtained at four repeats of a same scan angle at -8.0° throughout the length of the test, used to correct for the SIS-100 radiance source drift for M1 at HAM A side. Multiple lines are for different detectors.

The reason that NICST produces larger fitting residuals is still unclear. Possible errors caused by a drift correction for the SIS-100 radiance outputs were examined. During the RVS test, there are four repeats of a single scan angle at -8.0°. These repeats give us a measure of the total drift in the response measurement during the course of the test. Figure 6 compares drift corrections made between the linear and quadratic fits for M1. Both fits produces similar error bars with a maximum at 0.10%. Thus, errors in the drift correction are much smaller than the RVS fitting residuals. Thus it is unlikely that the larger RVS fitting residuals are caused by the drift corrections.

4. SUMMARY

This document provides the RVS results of the reflective solar and thermal emissive bands obtained from three independent groups: NICST, Raytheon, and the Aerospace Corporation. The RVS results are derived using a 2nd order polynomial fit to response measurements versus the angle of incidence. A comparison of the RVS is conducted for each band, detector, and HAM side. The RVS fitting residuals are examined and compared with the relative differences in RVS between independent studies. Results show that agreement between groups is within 0.1% for all bands except for one reflective solar band M9, where a difference of 0.2% is found due to use of the atmospheric water vapor correction for air conditions during the test by Raytheon. The fitting residuals are generally within 0.1% for all bands and comparable in magnitude with the relative differences in RVS found between groups.

ACKNOWLEDGEMENTS

REFERENCES

1. "National Polar-orbiting Operational Environmental Satellite Systems (NPOESS) Preparatory Project (NPP) Instrument Calibration and Support Element Design Document," NASA/GSFC, January 10, 2008, unpublished.
2. Xiong, S., H. Oudrari, D. Moyer, J. Sun, and N. Che "Response vs. Scan Angle of VIIRS EDU TEB (FP-10, part 2) Moderate bands". NICST_MEMO_05_016, December 16, 2005.
3. Pan, C. and N. Che, "SIS100 monitor data impacts on VIIRS FU1 Response Versus Scan (RVS) for the Reflective Solar Bands from FP-10", NICST_MEMO_08_006, February 28, 2007.
4. Moyer, D. and K. Rausch, "Preliminary FP-10 Part 2 TEB Response Versus Scan Results". October 10, 2007.
5. Ranshaw, C., "VIIRS FU1 Test Analysis Report for FP-10 Part 1, Reflective Band Response vs. Scan Angle (Version 2)", Raytheon Report Y24182, February 19, 2008.
6. Ranshaw, C., "VIIRS FU1 Test Analysis Report for FP-10 Part 2, Emissive Band Response vs. Scan Angle (Version 2)", Raytheon Report Y24007, February 18, 2008
7. Xiong, S., C. Pan, and N. Che, "Response vs. Scan Angle for VIIRS FU1 TEB (FP-10, part 2)". NICST_MEMO_08_008, March 10, 2008.
8. Wu, A., "Comparison of VIIRS SDR RVS and fitting uncertainty", NICST_REPORT_10_019, October 12, 2010.
9. Cronkhite J. and A. Wu, "Updated Analysis Results for VIIRS FU1 response Versus Scan Angle (RVS) for FP-10 TEB", NICST_MEMO_10_026, October 8, 2010.
10. "Response vs. Scan Angle (FP-10) Test Procedure for VIIRS (TP154640-250)", Raytheon, May 24, 2007.
11. "VIIRS Sensor Performance Verification Plan (TP154640-101 Rev. A)", Raytheon.